EFFECTS OF MESOPOROUS SILICA ON PMMA / SBA-15 COMPOSITES PREPARED BY EMULSION POLYMERIZATION

F.A. Zhang[1*], Z.J. Chen[1], Z.B.Wei[1], R.Bai[1], C.L.Yu[2]

[1]*College of Materials Science and Engineering, Guilin University of Technology, Guilin, China*
[1]*College of Chemical and Biochemical Engineering, Guilin University of Technology, Guilin, China*
*zhangfaai@glite.edu.cn

Keywords: Polymer Composite, Mesoporous Silica, Morphology, Emulsion Polymerization.

Abstract

PMMA composites were prepared through in-situ emulsion polymerization of methyl methacrylate in the presence of mesoporous silica SBA-15 with different morphologies. For composites containing rod-like mesoporous silica, the most decomposition temperature, the storage modulus, and glass transition temperature for the PMMA composite increased significantly, whereas the composite containing the mesoporous silica SBA-15 with sphere-like exhibited less improvement in comparison to pure PMMA. All the composites with mesoporous silica displayed higher mechanical properties in the high temperature. The introducing of mesoporous silica to PMMA decreased the dielectric constants of the polymer composites.

1 Introduction

Since mesoporous molecular sieves, hexagonally ordered mesoporous silicas M41S, were discovered at the beginning of the 1990s, the synthesis and application of advanced mesoporous materials has undergone rapid growth. Due to the large surface area, ordered pore structure and readily controlled pore diameters, ordered mesoporous silica has been believed the promising materials as catalysts, adsorbents, optical devices, and sensor devices[1-3].

Recently, researchers applied mesoporous silica as enhancement for polymer composite [4-15]. Jiao used mesostructured forms of silica as an effective reinforcing agent for a rubbery epoxy polymer, the reinforcement provided by mesostructures with larger pores were superior to those with smaller pore derivatives, most likely because of more efficient polymer impregnation of the particle mesopores [15]. Lin prepared brominated epoxy resin composites containing various amounts of SBA-15 and SBA-16 types mesoporous silicas, and found that the dielectric constant could be reduced due to the incorporation of the air voids stored within the mesoporous silica materials, thermal properties and mechanical properties were also improved by incorporation of the mesoporous silica materials [8]. Poly(methyl methacrylate)/ mesoporous molecular sieve (PMMA/MMS) composites were prepared by in situ polymerization. The thermal stability, glass transition temperatures, tensile strength and Young's modulus of the composites increase with the increasing concentration of MMS. Due to the interpenetrating of organic polymer chain with inorganic scaffold, the interface interaction between the surface of inorganic particles and the polymer resin was improved [9].

Emulsion polymerization is an attractive technology for preparing PMMA and composites. We have prepared PMMA mesoporous composites via batch emulsion polymerization and compression molding [16] using a large pore MSU-F silica with a mesocellular foam structure, and found that the thermal stability, glass transition temperature, mechanical properties were improved considerably, in comparison to pure PMMA. The Effect of framework structure and pore size of the mesoporous silica, MCM-41, MCM-48 and MSU-F, as well as the preparation methods on thermomechanical properties were investigated [5].

The aims of the paper was to prepare PMMA mesoporous composites via emulsion polymerization method using mesoporous silica with different morphology, rod-like, ball-like with small or large pore size, and investigate the effects of mesoporous silica types on the monomer conversion, coagulum, molecular weight and distribution, thermal stability, mechanical properties and dielectric properties of the resulting composite.

2 Materials and testing methods

2.1 Materials

Methyl methacrylate (MMA), ammonium peroxydisulfate (APS), sodium dodecylsulfate (SDS), sodium bicarbonate ($NaHCO_3$) were all analytical grade reactants, purchased from Xilong Chemical Plant in Shantou, Guangdong province (China). Emulsifier polyoxyethylene nonyl phenol ethers (OP-10) was provided by Kelong Chemical Plant in Chengdu, Sichuan (China). In these materials, MMA was distilled under reduced pressure and APS was treated by recrystallization prior to use, respectively. Deionized water was used in all the experiments. Mesoporous silica was prepared according to literatures [17-18].

2.2 Preparation of PMMA composite by in-situ emulsion polymerization

Emulsion polymerization was carried out in a 250 ml glass reactor equipped with a reflux condenser, stainless-steel stirrer, nitrogen gas inlet and thermometer. The solid content of the emulsion was designed as 40% by weight. In the batch emulsion polymerization procedure, water (30 g), monomer MMA (20 g), OP-10 (0.4 g), SDS (0.4 g), $NaHCO_3$ (0.07 g), APS (0.1 g), and mesoporous silica (0.5 g) were charged into the reactor in the order stated. At the beginning of the polymerization, the reaction vessel was sonicated for 20 min, followed by degassing with nitrogen for 20 min, and then the system was heated to 75 ^{o}C for 3h. In the semi-continuous emulsion polymerization process, the raw material was added to the system dropwisely. Thus, PMMA emulsion was obtained. After that, the emulsion was demulsified by addition of a 10% aqueous solution of $Al_2(SO_4)_3$. The solid product was filtered, washed thoroughly with water, and finally dried at 60 ^{o}C in a vacuum oven for 24 h.

2.3 Characterization

The monomer conversion and coagulum were determined gravimetrically. The N_2 adsorption-desorption isotherms were obtained by using a Quantachrome NOVA 1200e Series at 77.35K. The molecular weight and molecular weight distribution of the polymers were measured on a Model 270 gel permeation chromatography (GPC) equipped with T6000 microstyragel columns at 30 ^{o}C, molecular weights were calibrated based on polystyrene standards, THF was used as an eluent at a flow rate of 1.0 ml/min. The morphology of these composites was observed with the scanning electron microscope (JEOL Ltd, Japan). The dielectric constants

of the composite films with dimension of 1cm×1cm were measured on a WY2851-type LCR bridge meter (Shanghai Wuyi electronics Co., Ltd., China) in the frequency range of 40 Hz to 1.0E6 Hz. Tan δ and storage modulus (E') were obtained by TA DMA Q500 instrument in a film tensile mode from 30 to 180 ^{o}C. The heating rate was set as 3 ^{o}C/min, and at a fixed frequency of 1 Hz. Samples were pressed into sheets at 240 ^{o}C for 30 min under 20000 psi pressure, and then cut to 30×6.5×0.4 mm^{3} specimens. The same instrument was used to conduct stress–strain experiments. The strain rate was set 0.1 % at 30 ^{o}C. NETZSCH STA 449C analyzer operated in N$_2$ over the temperature range 30–600 ^{o}C provided thermogravimetric analysis (TGA) curves. The heating rate was 10 ^{o}C /min. NETZSCH DSC 204 differential scanning calorimeter (DSC) afforded T$_g$ of the composites under a nitrogen atmosphere. The scan rate was 10 ^{o}C /min over the temperature range 30–180 ^{o}C. T$_g$ values for composites were determined from the second scan of the DSC curve.

3 Results and Discussions

3.1 Preparation and characterization of mesoporous silicas

Rod-like SBA-15 and sphere-like SBA-15 with small pore and large pore were prepared by hydrothermal methods and defined as SBA-15 (R), SBA-15 (S) and SBA-15 (L), respectively. It was seen from the SEM pictures in Fig.1 that the morphologies of these mesoporous SBA-15 were rod-like (A), or ball-like (B and C). They showed typical Langmuir IV absorption-desorption curves (Fig.2), the specific surface areas and pore sizes for SBA-15 (R), SBA-15 (S) and SBA-15 (L) were 456, 602, 762 m^{2}/g and 5.8, 6.5, 23.7 nm, separately. The results confirmed that the expected mesoporous silica were prepared successfully.
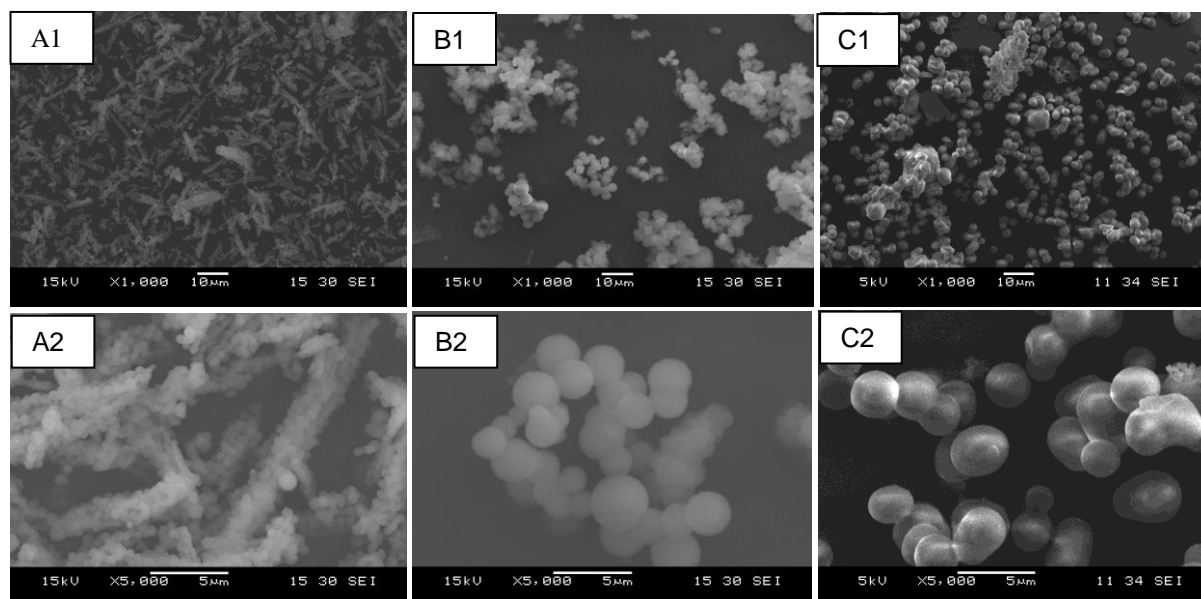

Fig. 1. SEM of different mesoporous materials (A:SBA-15(R),B:SBA-15(S),C: SBA-15(L))

3.2 Emulsion polymerization in the presence of mesoporous silica

Batch and semi-continuous emulsion polymerizations were carried out in the presence of mesoporous silicas with different morphology. The results showed that in all the experiments the monomer conversions were over 99% (Table 1), which indicated that the adding the mesoporous silica did not affect the monomer polymerization. However, the coagulum formed were varied greatly, the mesoporous silica with large pore produced more of the coagulum. This was caused by mesoporous silica adsorbing of emulsifier, the larger pore size

of the mesoporous silica, the more adsorption of the emulsifier, thus the higher critical micelle concentration (CMC) of the emulsifier. These were confirmed by the data obtained from CMC determination in Table 1. In addition, more of the coagulum was produced in the batch emulsion polymerization than in the semi-continuous emulsion polymerization due to the less stability in the former process in which all the materials were added together.
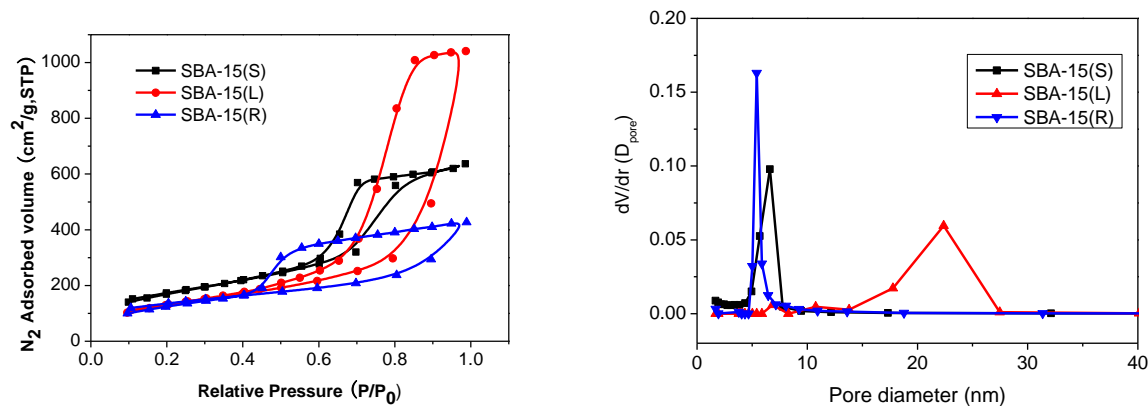

Fig. 2. Pore volume and pore size of different mesoporous materials

Types	Conversion/%		Coagulum/%		CMC /mmol/L
	Batch	**Semi-continuous**	**Batch**	**Semi-continuous**	
PMMA	99.9	99.9	0.5	0.5	4.78
PMMA/SBA-15(R)	100.0	99.5	2.3	0.6	5.04
PMMA/SBA-15(S)	99.7	99.9	4.2	0.6	7.55
PMMA/SBA-15(L)	100.0	99.8	6.3	1.4	8.29

Table 1. Effects of different structure of mesoporous materials on the emulsion polymerization

The molecular weights and molecular weight distributions of the PMMA composites obtained from MMA emulsion polymerization in the presence of mesoporous silica were determined and displayed in Table 2. It showed that the number-average molecular weight (M_n) decreased remarkably, while weight-average molecular weight (M_w) did not changed much, upon the introduction of mesoporous silica into the emulsion polymerization system. Accordingly, the molecular weight distribution index (M_w/M_n) increased greatly. However, the M_n of the PMMA polymerized in the system containing mesoporous silica was similar. The increase of the CMCs of the emulsifier might account for the decrease of the M_n partly which decreased the number of micelle in the system thus lower M_n.

Types	M_w	M_n	M_w/M_n
PMMA	223493	113677	1.97
PMMA/SBA-15(R)	207178	70225	2.95
PMMA/SBA-15(S)	190527	60349	3.16
PMMA/SBA-15(L)	224454	70546	3.18

Table 2. Effects of structures of mesoporous materials on the molecular weight and its distribution

3.3 TG and DSC analysis of the PMMA mesoporous composites
The thermal stabilities and glass transition temperature (T_g) of the PMMA mesoporous composites were given in Fig. 3. The PMMA composite with SBA-15 (R) exhibited the greatest improvement in thermal stability while the composite with SBA-15 (S) reduced the

thermal stability a little which low the most decomposition temperature. Rod-like mesoporous silica hindered the heat transfer more efficiently thus enhanced the thermal stability. The T_g's of the composites were all increased, again, the polymer composite with rod-like SBA-15 exhibited the highest T_g value (increased 20 ^{o}C, in compared with pure PMMA) which mean that the movement of the polymer chain was hindered and more energy was needed to make this movement. Additionally, the pore size of the ball-like mesoporous silica on the T_g of the composite was ignored.
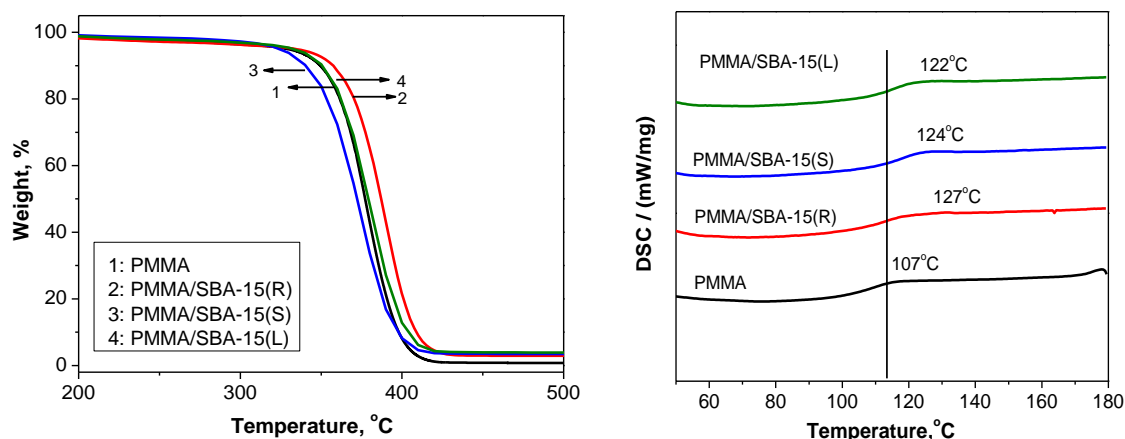

Fig. 3. TG and DSC curves for PMMA/ mesoporous composites

3.4 Mechanical properties of the PMMA mesoporous composites

The dynamic mechanical properties of the PMMA mesoporous composites were provided in Fig. 4A which illustrated that the composite with rod-like SBA-15 exhibited the highest storage modulus both in ambient and high temperature, whereas the composite containing sphere-like SBA-15 improved the storage modulus in the high temperature only. This indicated that the adding of the rod-like mesoporous silica hindered the heat transfer and dispersed the stress evenly, just like the fiber in the composite. The peak temperature in the loss factor curve (Fig. 4B) is the T_g value of a polymer, which indicated that rod-like SBA-15 increased the T_g most, while ball-like SBA-15 increased the T_g a little. The rod-like SBA-15 hindered the movement of polymer chains resulting in high T_g value. The stress-strain curves in Fig. 5 also illustrated that the rod-like SBA-15 improved the Young's modulus of the polymer based on the same reason, while ball-like SBA-15 with small pore size did not improve the Young's modulus.
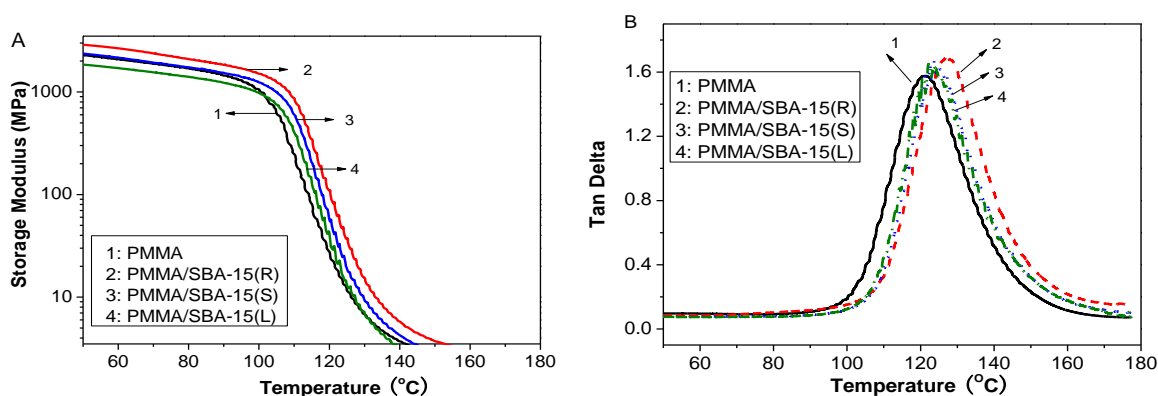

Fig. 4. The storage modulus and Tan delta curves of PMMA/mesoporous composites

3.5 Dielectric properties of the PMMA mesoporous composites

The dielectric constant of the PMMA composite was determined within a certain frequency range and given in Fig. 6. It showed that the dielectric constant of the composite decreased upon the introduction of mesoporous silica into the polymer. It is well known that the void in the composite accounts for the decrease of the dielectric constant. The ball-like SBA-15 with large pore size (23.7 nm) introduced the maximum amount of voids into the polymer resulting in the minimum dielectric constant of the polymer. On the contrary, the rod-like SBA-15 with small pore size decreased the dielectric constant the least due to few void was introduced. The voids in the polymer composite also contributed for the less improvement in the mechanical properties of the composite.
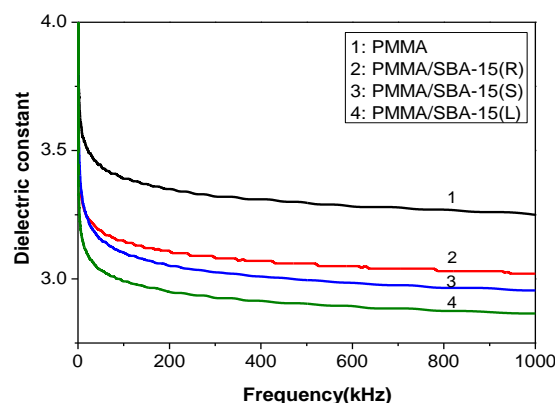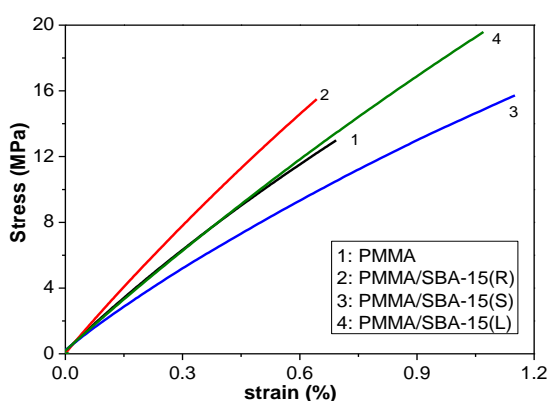
Fig. 5. Stress-strain curves of PMMA composite films   **Fig. 6.** Dielectric constant of PMMA composite films
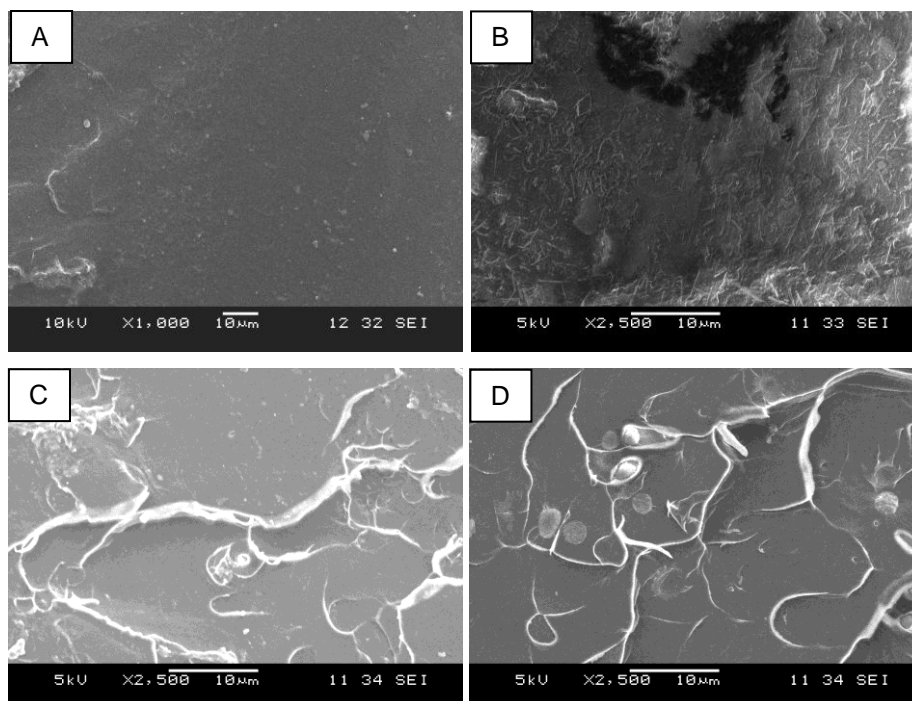

Fig.7. SEM images of the PMMA/mesoporous composite films (A:PMMA, B:PMMA/SBA-15(R),C: PMMA/SBA-15(S), D: PMMA/SBA-15(L))

3.6 Morphology of the PMMA mesoporous composites films

SEM images of the polymer composite films in Fig. 7 displayed that the surface of PMMA was smooth (Fig. 7A), and a great amount of the rod-like SBA-15 particle (Fig. 7B), which

were dispersed evenly in the polymer composite, could be seen on the surface of the PMMA/SBA-15 (R) composites which accounted for the improvement in mechanical properties of the polymer composites. On the contrary, a long strip-like protuberances and some of ball-like particles were seen both on the surface of PMMA/SBA-15 composites (Fig. 7C and D), regardless of incorporating SBA-15 with large or small pore size. These not well dispersed particles did not improve the mechanical properties of the composite much.

4 Conclusions

PMMA mesoporous composites containing the rod-like SBA-15 or ball-like SBA-15 with large or small pore size were prepared successfully from *in-situ* emulsion polymerization. The introduction of the SBA-15 particle had no effects on the monomer conversion, but increased the coagulum content and decreased the number-average molecular weight of the polymer resulting in higher polydispersity index due to the adsorption of emulsifier to the channel of mesoporous silica. The incorporation of rod-like SBA-15 into PMMA provided for the polymer composite the greatest improvement in thermal stability, glass transition temperature and mechanical properties, while the introduction of ball-like SBA-15 only gave rise to a little improvement in all these properties. The morphology of the polymer composite confirmed that the SBA-15 particles were incorporated into the polymer. The dielectric constants of the polymer composites were decreased, the composite containing SBA-15 with large pore size exhibited the lowest dielectric constants which suggested that a lot of voids were existed in the composites.

References
[1] Zeng C.N., Han S.H., Yan X., Yu X.J., Che H.W., Zhao X.H. Ordered mesoporous silica/polyaniline composites. *Progress in Chemistry,* **20**, pp.26-32 (2008).

[2] Song Y., Li Y.H. The application of mesoporous molecular sieves. *Progress in Chemistry,* **19**, pp.659-664 (2007).

[3] Lin H.P., Cheng Y.R., Lin C.R., Li F.Y., Chen C.L., Wong S.T., Cheng S.F., Liu S.B., Wan B.Z., Mou C.Y., Tang C.Y., Lin C.Y. The synthesis and application of the mesoporous molecular sieves MCM-41 - A review. *J Chin Chem Soc,* **46**, pp.495-507 (1999).

[4] Jiao J., Sun X., Pinnavaia T.J. Reinforcement of a rubbery epoxy polymer by mesostructured silica and organosilica with wormhole framework structures. *Adv Funct Mater,* **18**, pp.1067-1074 (2008).

[5] Zhang F.A., Song C., Yu C.L. Effects of preparation methods on the property of PMMA/SBA-15 mesoporous silica composites. *Journal of Polymer Research,* **18**, pp.1757-1764 (2011).

[6] Zhang F.A., Lee D.K., Pinnavaia T.J. PMMA/mesoporous silica nanocomposites: Effect of framework structure and pore size on thermomechanical properties. *Polymer Chemistry,* **1**, pp.107-113 (2010).

[7] Wang N., Zhao C.L., Shi Z.X., Shao Y.W., Li H.W., Gao N. Co-incorporation of MMT and MCM-41 nanomaterials used as fillers in PP composite. *Materials Science and Engineering B-Advanced Functional Solid-State Materials,* **157**, pp.44-47 (2009).

[8] Lin J.J., Wang X.D. Preparation, microstructure, and properties of novel low-kappa brominated epoxy/mesoporous silica composites. *Eur Polym J,* **44**, pp.1414-1427 (2008).

[9] Run M.T., Wu S.Z., Zhang D.Y., Wu G. A polymer/mesoporous molecular sieve composite: Preparation, structure and properties. *Mater Chem Phys,* **105**, pp.341-347 (2007).

[10] Lin J., Wang X. Novel low-[kappa] polyimide/mesoporous silica composite films: Preparation, microstructure, and properties. *Polymer,* **48**, pp.318-329 (2007).

[11] Lenarda M., Chessa G., Moretti E., Polizzi S., Storaro L., Talon A. Toward the preparation of a nanocomposite material through surface initiated controlled/"living" radical polymerization of styrene inside the channels of MCM-41 silica. *Journal of Materials Science,* **41**, pp.6305-6312 (2006).

[12] Cheng Q., Pavlinek V., Lengalova A., Li C., He Y., Saha P. Conducting polypyrrole confined in ordered mesoporous silica SBA-15 channels: Preparation and its electrorheology. *Microporous Mesoporous Mater,* **93**, pp.263-269 (2006).

[13] Tian B.S., Yang C. Preparation and characterization of thermo-sensitive mesoporous PNIPAAm/SBA-15 composite. *Acta Chim Sinica,* **66**, pp.505-510 (2008).

[14] Park J.H., Lee Y.H., Oh S.G. Preparation of thermosensitive PNIPAm-Grafted mesoporous silica particles. *Macromol Chem Phys,* **208**, pp.2419-2427 (2007).

[15] Jiao J., Sun X., Pinnavaia T.J. Mesostructured silica for the reinforcement and toughening of rubbery and glassy epoxy polymers. *Polymer,* **50**, pp.983-989 (2009).

[16] Zhang F.-A., Lee D.-K., Pinnavaia T.J. PMMA-mesocellular foam silica nanocomposites prepared through batch emulsion polymerization and compression molding. *Polymer,* **50**, pp.4768-4774 (2009).

[17] Zhao D.Y., Feng J.L., Huo Q.S., et al. Triblock copolymer syntheses of mesoporous silica with periodic 50 to 300 angstrom pores. *Science*, **279**, pp.548-552(1998).

[18] Wang L.N., Qi T., Zhang Y., Chu J.L. Morphosynthesis route to large-pore SBA-15 microspheres. *Microporous and Mesoporous Materials*, **91**, pp.156–160(2006).